Hydro-climatology: Variability and Change (Proceedings of symposium J-H02 held during IUGG2011 in Melbourne, Australia, July 2011) (IAHS Publ. 344, 2011).

Assessment of flash flood events using remote sensing and atmospheric model-derived precipitation in a hydrological model

ISMAIL YUCEL[1] **& FATIH KESKIN**[2]

1 *Middle East Technical University, Civil Engineering Department, Ankara 06531, Turkey*
iyucel@metu.edu.tr

2 *State Hydraulic Works, Ankara, Turkey*

Abstract Remotely-sensed precipitation estimates and regional atmospheric model precipitation forecasts provide rainfall data at high spatial and temporal resolutions with a large-scale coverage, and can therefore be potentially used for hydrological applications for making flash flood forecasts and warnings. This study investigates the performance of the rainfall products obtained from the Hydro Estimator (HE) algorithm of NOAA/NESDIS and the Weather Research and Forecasting (WRF) model, and their use in a hydrological model (HEC-HMS) to simulate the catastrophic flood events which occurred in the Ayamama basin in northwest Turkey during 7–12 September 2009. The WRF model is also run with three-dimensional variational assimilation to obtain improved precipitation forecasts. The precipitation estimates at 4-km from the HE and WRF model, with and without assimilation, were evaluated against raingauge and radar data. The 4-km HE and WRF-estimated rainfall showed capabilities in capturing the timing of the flood events and to some extent the spatial distribution and magnitude of the heavy rainfall. Hydrological modelling based on HEC-HMS is applied using rainfall data from raingauges, radar, HE and WRF model. By use of surface hydrographs obtained from HEC-HMS, the HEC-RAS hydrological model is used to simulate inundation extent. The extent of the inundated areas in the river basin changes according to the peak discharges of the surface hydrographs used in the HEC-RAS module.

Key words satellite rainfall; radar; hydrological model; flash flood; Turkey

INTRODUCTION

Floods are among the most recurring and devastating natural disasters and are responsible for significant loss of life and property throughout the world. This is especially significant in developing countries, where precipitation data are poor, communication is slow and evacuation is difficult. Additionally, precipitation gauges are generally clustered in urban areas and ground-based radar is often blocked by mountains. This leaves large tracts where little or no data is gathered. In data-sparse regions, alternative products such as model forecasts and remotely-sensed data should be used for flood forecasting and warning issues, as they provide more continuous monitoring of precipitation data both spatially and temporally over a large coverage extent. Hydrological model simulations depend heavily on the availability of reliable precipitation estimates. These aforementioned difficulties in estimating precipitation impose an important limitation on the possibility and reliability of hydrological forecasting and early warning systems. Therefore, as a supplement to raingauge and radar rainfall data, the use of remotely sensed and numerical model-based precipitation products becomes critical in hydrological simulations. The main objective of the present study is to investigate the feasibility of making hydrological diagnostics for a catastrophic flood event which occurred in a small basin located in northwestern Turkey using the capabilities of a hydrological model forced by raingauge, radar, remotely-sensed and mesoscale atmospheric model precipitation products.

Heavy precipitation events occurred during the period 7 to 11 September in 2009 and resulted in accumulated rainfall totals of approximately 10 times the long-term average precipitation in Istanbul, Turkey, during the month of September. As a hydrological response, the severe rain events triggered the worst flooding in decades in the region during which at least 24 people died in Istanbul, and there were seven deaths elsewhere in northern Turkey, in addition to significant damage to property. In this study, the applicability and accuracy of the Hydro Estimator (Scofield & Kuligowski, 2003) and Weather Research and Forecasting (WRF)-derived precipitation is tested along with the radar and raingauge precipitation data. Moreover, the utility of these rainfall products in estimating flood hydrographs using the Hydrologic Engineering Center's Hydrological

Modeling System (HEC-HMS) is examined. The Hydrologic Engineering Center's River Analysis System (HEC-RAS) is also used to display inundation maps using forcing rainfall from radar, raingauge, HE, and WRF model.

STUDY AREA, DATA, MESOSCALE ATMOSPHERE AND HYDROLOGICAL MODELLING

The study area, together with raingauge and radar positions located in the northwest region of Turkey, is shown in Fig. 1. The Ayamama basin, for which hydrological modelling is applied, is also shown in Fig. 1. The study area is impacted by polar air masses of continental origin (Icelandic Low and cold Siberian High) in the winter and by subtropical air-masses (Azores High and part of the Monsoon Low) in summer. When the Siberian High crosses the Black Sea approaching the northern coasts of Turkey, cold, and dry air turns into a maritime continental air-mass due to the acquired moisture content. The diversity of the geographic structure, extent of the mountains, and effects of the seas in the vicinity of the land, determine the climate types of the region.

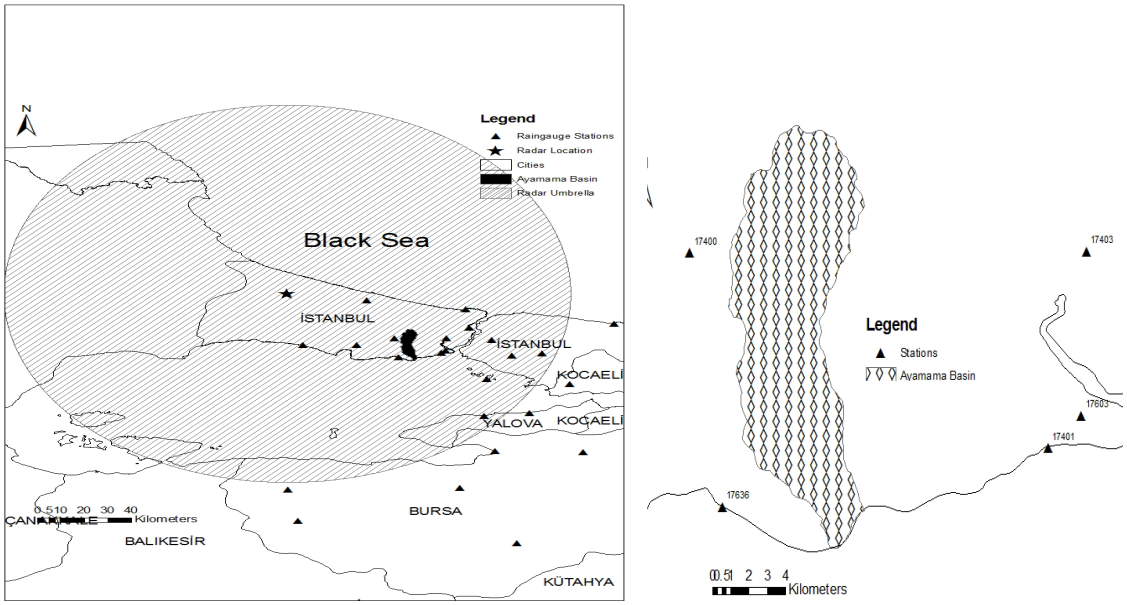

Fig. 1 Study area and the locations of the Ayamama basin, radar and raingauge stations.

The hourly rainfall data obtained from the 34 raingauges at the automated weather stations are used for comparison with the HE and radar data. The HE computes real-time quantitative precipitation estimates of instantaneous rain rate from 10.7-μm brightness temperatures with modifications to the resulting rain rate using numerical weather model data to account for sub cloud evaporation and other effects (Scofield, 2001). The HE provides precipitation data with high spatial resolution, 4 km, and a temporal resolution of 15 minutes. Since analyses are performed at hourly time intervals the HE estimates are also converted to hourly values. The radar data have a 6–10 minute time interval which is converted to an hourly interval. In the study, hourly measurements from 52 raingauge stations are included in the rectangular frame described by a region covering longitudes 25.53–30.27E, and latitudes 39.19–41.48N. The 34 stations are used for the accuracy assessment under the radar umbrella, which is a circle having a radius of 120 km from the radar location.

As a mesoscale model, the WRF modelling system (version 3.3, Chen & Dudhia, 2001), with a nested configuration at 12 km and 4 km domains, is applied to provide precipitation data as forcing for the hydrological model. The 4-km rainfall products at the 1-hour time interval is used

from WRF, for which initial and boundary conditions are provided from the European Centre for Medium Range Weather Forecasts (ECMWF) at 25 km. In addition, with the use of a three-dimensional variational data assimilation technique (3D-Var) the initial structure of the regional hydrometeorology is more reliable, and therefore improved precipitation depiction and the skill in hydrological forecasting can be expected.

The hydrological response of the Ayamama basin to flood events is produced using the HEC-HMS runoff model. An independent sample of events is used to calibrate the HEC-HMS in terms of soil behaviour (losses and imperviousness), which exerts a fundamental role over the runoff volume. In a steady-state mode, the peak discharge of the flood hydrographs is imported into the HEC-geoRAS program to determine the extent of the flooded water along the river basin.

RESULTS

Comparison of precipitation products

Figure 2 shows area-averaged precipitation from WRF with and without assimilation, HE, radar, and raingauge data for the whole event period 8–12 September 2009. All rainfall products underestimate the observed rainfall amount by various magnitudes, especially for heavy precipitation events, along with the event periods. This underestimation is more significant for the WRF model, whether it is used with a 3D-Var technique or not. However, the WRF, HE and radar estimates captured better the timing of the observed events and fluctuations in rainfall through the event period than the rainfall magnitude. Satellite estimates and radar observations tend to follow temporal variations of precipitation more accurately compared to the WRF model. The spatial variability of precipitation is responsible, to some extent, for the underestimation in area-average precipitation, as shown in Fig. 2.

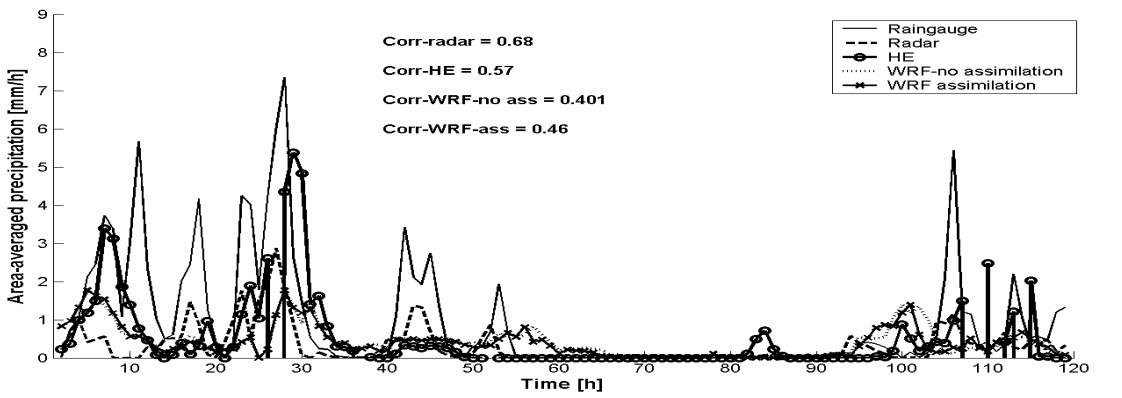

Fig. 2 Comparison of area-averaged precipitation derived from radar, HE, and WRF with and without assimilation and observation for all event period from midnight of 8 September to midnight of 12 September 2009. Correlation coefficients between estimated and gauged rainfall are also given.

The level of accuracy of rainfall products is described by the correlation coefficient values between the WRF and raingauge (0.46 with 3D-Var and 0.401 without 3DVar), between HE and raingauge (0.57) and between radar and raingauge rainfall (0.68). Because insignificant changes are provided by the assimilation, rainfall from WRF with 3D-Var is used in all analyses. The underestimation also appears in the scatter plots shown in Fig. 3, when observed and estimated rainfall are inter-compared by using point values of hourly, daily and event-total rainfall. However, the uncertainty is greatly reduced when aggregating rainfall values in temporal scale from hourly to total event period (4 days). The related statistics show higher correlation coefficients and less error and bias for daily and total events for all products. The superior performance of the radar and satellite rainfall estimates to WRF-derived rainfall is also evident from the scatter plot analysis.

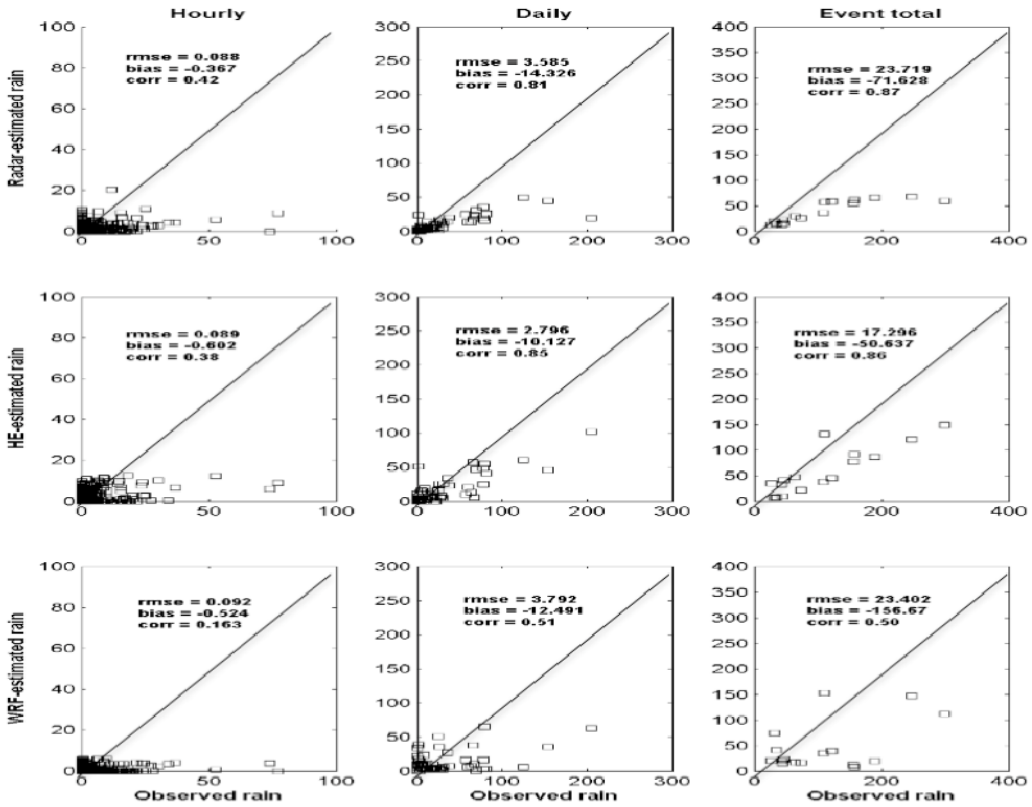

Fig. 3 Scatter plots between radar-, HE-, and WRF-derived rainfall and observation for hourly (mm h^{-1}), daily (mm d^{-1}) and event total rainfall (mm 4-d^{-1}). Related statistics, root mean square error (rmse), bias, and correlation coefficient (corr) are also given.

Utility of the HE, Radar, WRF, and Raingauge data for hydrological modelling

The hydrological response of Ayamama basin to the catastrophic flood event is investigated using the HEC-HMS model based on the SCS Curve Number method with rainfall forcing data from raingauge, HE, radar, and WRF with and without 3D-Var. Hourly rainfall values from each source falling within the basin, together with land use and soil types data, are used to calculate SCS curve-number unit hydrographs. According to the land-use type, the basin is divided into three different categories, and depending on the soil type of each land use, three different curve numbers are calculated. The higher curve number indicates higher surface runoff and less infiltration losses. The curve numbers for urban and rural areas in Ayamama basin were calculated as 88 and 49, respectively. The topography, slope and sub-basins of Ayamama basin are shown in Fig. 4, while some basin characteristics are given in Table 1.

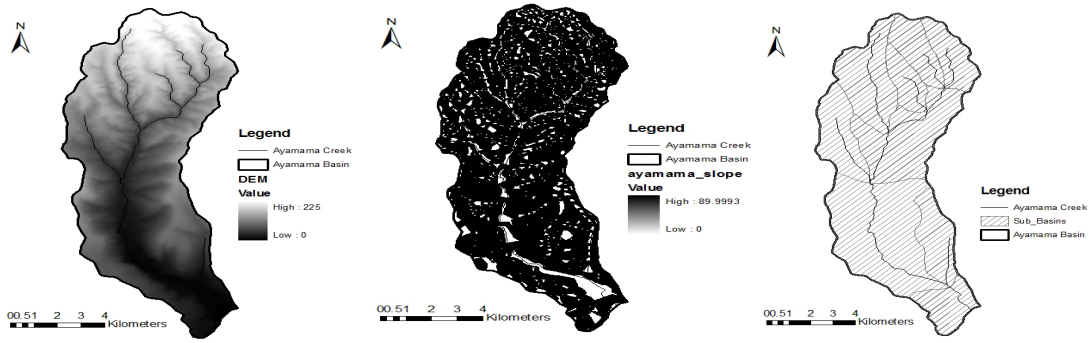

Fig. 4 Topography, slope and sub-basins of Ayamama basin, respectively.

Table 1 Basin characteristics.

Mean slope	Mean elevation	Accumulation time	Longest stream length	Basin area
6.94 %	86,64 meter	7.11 hour	41.314 km	71.02 km^2

The curve number for each sub-basin was calculated by aggregating the pre-determined curve number values. Finally, a basin-averaged curve number of 65 and basin characteristics given in Table 1 are used in HEC-HMS to simulate surface runoff hydrographs. The resulting surface runoff hydrographs and the basin-averaged hourly rainfall hyetographs for the raingauge, radar, HE and WRF model rainfall data sets are shown in Fig. 5(a), (b), (c) and (d), respectively.

Peak discharge values of 264.7 m^3/s, 159.8 m^3/s, 250 m^3/s and 210 m^3/s were obtained from surface runoff hydrographs derived using the raingauge, HE, radar, and WRF-with 3D-VAR rainfall products, respectively. Heavy rainfall events appear in the study area during the early mornings of 8 and 9 September 2009 in all rainfall products, with various magnitudes. The catastrophic flood event that occurred in Ayamama basin in the early morning of 9 September was triggered by the wet antecedent soil moisture condition resulting from the heavy rainfall of 8 September. Raingauge and radar-derived rainfall products better follow this feature. However,

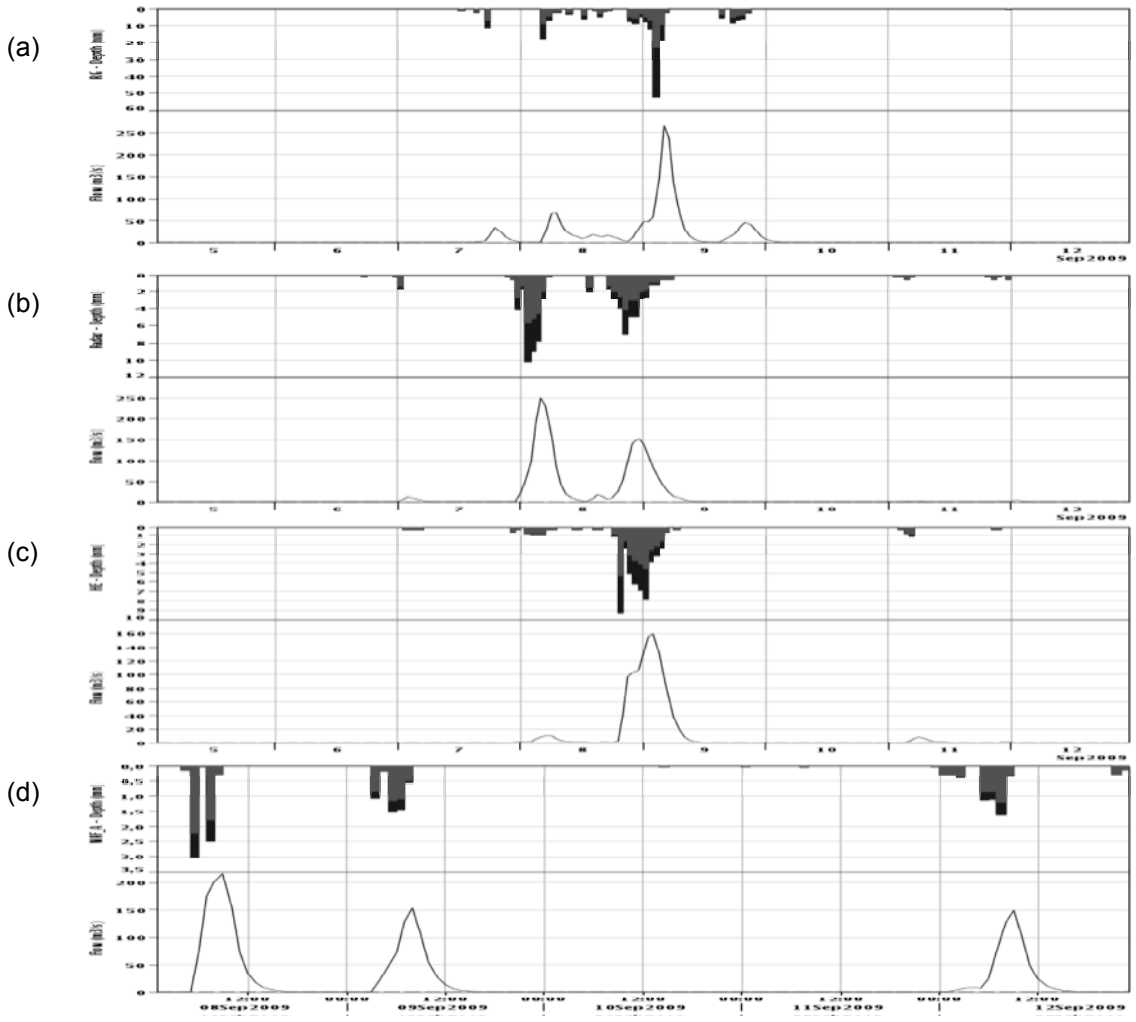

Fig. 5 HEC-HMS-simulated hourly surface runoff hydrographs and basin-averaged hourly hyetographs using rainfall data from raingauge (a), radar (b), HE (c), and WRF (d). The upper part of the hyetographs is excess rain contributing direct surface runoff. The time period for WRF model is from midnight 8 September to midnight 12 September, while it is from midnight 5 September to midnight 12 September for raingauge, radar and HE data.

the radar rainfall produced the highest discharge in early 8 September compared to the others. Discharge values caused the flood event early on 9 September are observable from all rainfall products, but with an underestimation compared to the discharge value calculated using raingauge data. For capturing the flood event on 9 September, the WRF-derived rainfall showed good skill (resulted peak discharge is 210 m^3/s) when compared to gauge data (resulting peak discharge 265 m^3/s). Nevertheless, the timing of the calculated flood discharge is captured well by all rainfall data sets. Overall, the differences between the rainfall products are also translated into the simulated surface runoff hydrographs throughout the event period.

Finally, the HEC-GeoRAS program was set up to determine the inundation maps along the stream. Using the peak runoff values for raingauge, HE, radar and WRF-derived rainfall in HEC-GeoRAS, the extent of inundation was calculated. Coverage by the flood water in the downstream close to the outlet is compared among the radar, gauge, HE and WRF rainfall in Fig. 6. Since all water eventually reaches the outlet of the basin, water coverage extends to the largest area downstream. Depending on the magnitude of the peak discharges, there are some differences between the areas of inundation shown in Fig. 6. In Fig. 6, the flooded area determined using the radar and gauge rainfall are similar to each other and larger than that obtained using the HE rainfall estimates. The WRF model also shows close approximation to the raingauge and radar flooded areas.

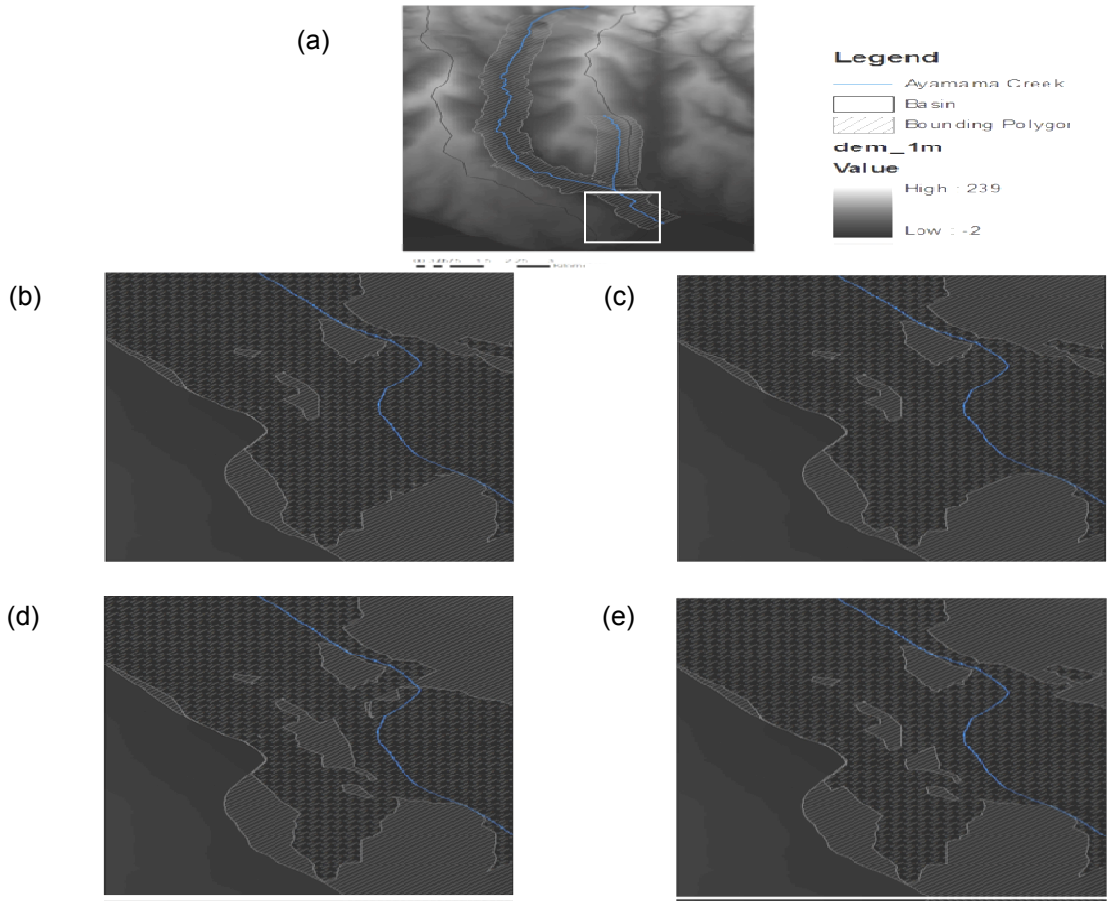

Fig. 6 A part of the inundation map located close to the outlet of the Ayamama basin is shown for the raingauge (b), radar (c), HE (d), and WRF (e) data, respectively. In (a), a general plan view of the Ayamama basin with a bounding polygon along with river and a bounding box to show the extent of inundation is displayed. A topographical map at 1-m resolution is used to generate inundation maps.

SUMMARY AND CONCLUSIONS

In this study, an evaluation is made to determine the representativeness of the magnitude and temporal variation of heavy precipitation events described by various sources: raingauges, radar, satellite and a mesoscale atmosphere model. The hydrological response of the Ayamama basin (Istanbul, Turkey) to heavy precipitation events, simulated using the aforementioned rainfall data in the HEC-HMS model, is investigated. The extent of the inundated areas for each data set is determined along the stream channel. Main conclusions from this study are drawn as follows:

- Rainfall estimates from radar, the HE and the WRF model underestimated the magnitude of the heavy precipitation events based on the comparison with raingauges. However, the timing of the rainfall events from the estimates matches well with observation. Underestimation is more significant with the WRF model whether the model is run with a 3D-Var technique or not. Uncertainty is greatly reduced as rainfall estimates are aggregated from hourly to total event period.
- Surface runoff hydrographs with various peak discharges were derived from each rainfall data set. Differences in rainfall amount affected the magnitude and the time of occurrence of the peak discharges. Relative to the gauge-derived hydrograph, the radar data produced a flood hydrograph of greater amplitude compared to the others. The surface runoff hydrograph determined from WRF-derived precipitation closely matches the primary peak discharge of the radar data. The flood hydrograph calculated by using the HE rainfall estimates follows the general behaviour of the gauge- and radar-retrieved hydrographs with lower discharge values.
- Depending on the magnitudes of the peak runoff values from each rainfall data set, the flood coverage areas show the greatest variability in the downstream close to the outlet of the basin. Among the data sets, the radar data showed the most similar extent of water coverage compared to the raingauge data.
- The sensitivity of the hydrological response of the Ayamama basin to the heavy precipitation events is successfully reproduced.

REFERENCES

Chen, F. & Dudhia, J. (2001) Coupling an advanced land surface-hydrology model with the Penn State-NCAR MM5 modeling system. Part I: Model implementation and sensitivity. *Mon. Weather Rev.* **129**, 569–585.

Scofield, R. A. (2001) Comments on "A quantitative assessment of the NESDIS Auto-Estimator". *Weather Forecasting* **16**, 277–278.

Scofield, R. A. & Kuligowski, R. J. (2003) Status and outlook of operational satellite precipitation algorithms for extreme-precipitation events. *Weather Forecasting* **18**, 1037–1051.